

Vision and Language Integration for Domain Generalization

Yanmei Wang^{a,b,c}, Xiyao Liu^{a,b}, Fupeng Chu^{a,b,c,1} and Zhi Han^{a,b,*}

^aState Key Laboratory of Robotics, Shenyang Institute of Automation, Chinese Academy of Sciences, Shenyang, 110016, China

^bInstitutes for Robotics and Intelligent Manufacturing, Chinese Academy of Sciences, Shenyang, 110169, China

^cUniversity of Chinese Academy of Sciences, Beijing, 100049, China

ARTICLE INFO

Keywords:

Domain generalization
vision language model
low-rank matrix
word vector.

ABSTRACT

Domain generalization aims at training on source domains to uncover a domain-invariant feature space, allowing the model to perform robust generalization ability on unknown target domains. However, due to domain gaps, it is hard to find reliable common image feature space, and the reason for that is the lack of suitable basic units for images. Different from image in vision space, language has comprehensive expression elements that can effectively convey semantics. Inspired by the semantic completeness of language and intuitiveness of image, we propose VLCA, which combine language space and vision space, and connect the multiple image domains by using semantic space as the bridge domain. Specifically, in language space, by taking advantage of the completeness of language basic units, we tend to capture the semantic representation of the relations between categories through word vector distance. Then, in vision space, by taking advantage of the intuitiveness of image features, the common pattern of sample features with the same class is explored through low-rank approximation. In the end, the language representation is aligned with the vision representation through the multimodal space of text and image.

1. Introduction

Deep neural networks have demonstrated significant performance in many applications Zhang, Rao, Huang, Li, Zhou and Zeng (2024); Tian, Li, Fu, Zhu, Yu and Wan (2024); Ge, Zhang, Wang, Coleman and Kerr (2023); Wu, Liu, Zhu, Wang and Zha (2021); Wu, Liu, Zha, Chen and Sun (2019a); Jia, Chow and Yuan (2024); Li, Cheng, Chen, Gao, Shi and Zeng (2024a); Lin, Bao, Huang, Li, Zheng and Chen (2024); Wu, Zha, Wen, Chen, Liu and Chen (2019b); Zhu, Liu, Wu, Wang and Zha (2020); Liu, Lv, Lee and Shen (2024). However, the training of neural networks is influenced by the distribution of the training data. Specifically, due to the fact that the number of parameters in deep neural networks far exceeds the number of samples, the network model tends to overfit the distribution of the training data, which leads to learning features that are specific to the distribution of the learned data. As a result, the model may perform poorly on data from other distributions. To address the aforementioned issues, domain generalization has attracted increasing attention. The aim of domain generalization is to train the network on source domains, enabling it to generalize effectively on unseen target domains.

The basic units in natural language processing (NLP) are words. Similar to words in language, the basic units in images can be seen as pixels. However, unlike words in language, pixels in the image do not possess explicit semantic concepts. They solely represent color information at a specific location within the image. Training a convolutional neural network (CNN) allows us to obtain a set of filters that serve as effective feature extractors. Extracted features can express the semantic information of an image. However,

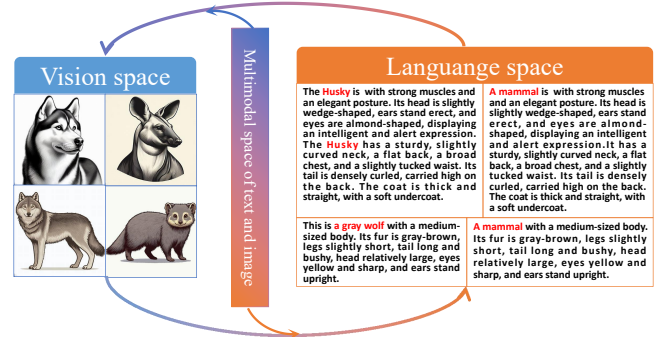


Figure 1: The ambiguity of the text descriptions in language space and the intuitiveness of images in vision space. The descriptions of Husky and gray wolf are generated by GPT-3.5 Floridi and Chiriatti (2020). The descriptions of the two are approximate. Then, we use the DALL-E Reddy et al. (2021) to generate the picture of Husky and gray wolf according to the descriptions, as shown in the two pictures of the first column. In the second column, the "Husky" and "gray wolf" in the text descriptions are replaced with "mammal", and the other descriptions remain unchanged, resulting in two other animals that fit the description. We attempt to combine language space and vision space and connect the multiple image domains by using semantic space as the bridge domain.

as mentioned earlier, neural networks can easily overfit the distribution of the training data when extracting features. This may lead to the extraction of domain-specific features, making it challenging to effectively capture features from other domains. For instance, image features such as color and texture extracted from the "photo" domain may not be applicable to the "sketch" domain, which primarily consists of simple outlines and strokes.

With the emergence and development of word vector Pennington, Socher and Manning (2014); Church (2017)

*Corresponding author

✉ hanzhi@sia.cn (Z. Han)

🌐 <https://orcid.org/0000-0002-8039-6679> (Z. Han)

ORCID(s):

and CLIP Radford, Kim, Hallacy, Ramesh, Goh, Agarwal, Sastry, Askell, Mishkin, Clark et al. (2021), applying semantic supervision from NLP to image processing has become possible. However, language is ambiguous. For instance, for someone who has never seen a dog or a wolf, we cannot effectively convey the characteristic differences between the two using language alone, as shown in Fig. 1. The descriptions of Husky and gray wolf are generated by GPT-3.5 Floridi and Chiriatti (2020) with the prompt “*What does a Husky look like?*”. Then, we use the DALL-E Reddy et al. (2021) to generate the picture of Husky and gray wolf according to the descriptions, as shown in the two pictures of the first column. However, when the “Husky” and “gray wolf” in the text descriptions are replaced with “mammal”, and the other descriptions remain unchanged, it results in two other animals in the second column, which also fit the descriptions. In contrast, images as a more advanced expression form than language, provide a more intuitive way to represent features.

Inspired by the above observations, to fully leverage the semantic completeness of language basic units and the intuitiveness of image features, we attempt to integrate the basic units of language with the explicit representation in vision, which means using semantic space as the bridge domain to connect multiple image domains so as to learn domain-invariant features. In language space, word vectors are used to supervise the relative relationships between categories. In vision space, the common patterns among samples of the same category are explored through matrix low-rank approximation. Following these, the multimodal space of text and images serves as a bridge to connect the language space and vision space. This is achieved by constraining the domain-specific information, making domain embedding and image features orthogonal.

The contributions of the method can be summarized as follows:

- Combining the advantages of completeness of language and intuitiveness of image features, multimodal semantic space is used as the bridge domain to propose a domain generalization method based on language and vision space.
- In multimodal space, the domain embedding of the domain prompt is constructed by CLIP, and then domain embeddings are constrained to be orthogonal to the image features, thereby reducing the influence of the domain variations.
- In the language space, the semantic distance is measured between classes through word vectors to provide interclass relationship supervision for network training.
- In vision space, low-rank decomposition is performed on the features matrix of the same category, and the features matrix is made approximate the subspace spanned by the largest singular value, so as to obtain common patterns of the same class samples.

2. Related Work

2.1. Domain Generalization

Domain generalization aims to address the performance degradation of a model when faces new, unseen domains or environments. In the real world, models are often trained on a specific dataset or environment, however, when the model is applied to a domain different from the training data, its performance can degrade significantly. There are many studies on domain generalization methods, including sample augmentation Chaari, Fekih, Seibi and Hmida (2018); Xu, Zhang, Zhang, Wang and Tian (2021); Kang, Lee, Kim and Kwak (2022); Li, Li, Tan and Liu (2024b), feature selection techniques Muandet, Balduzzi and Schölkopf (2013); Li, Pan, Wang and Kot (2018b); Dou, Coelho de Castro, Kamnitsas and Glocker (2019); Liu, Xiong, Li, Tian and Zha (2021); Niu, Yuan, Ma, Xu, Liu, Chen, Tong and Lin (2023); Zhou, Chen, Yang, Wang and Chaib-Draa (2023); Ng, Zhang, Zhong and Zhang (2024), and meta-learning methods Li, Yang, Song and Hospedales (2018a); Balaji, Sankaranarayanan and Chellappa (2018); Du, Xu, Xiong, Qiu, Zhen, Snoek and Shao (2020). Feature selection helps the model learn features that are common to all domains, reducing dependence on specific domains. Domain adaptation technology aims to effectively transfer knowledge between different domains by adjusting the parameters of the model. The meta-learning method simulates the situation in different domains during the training process to enhance the model’s adaptability to unknown domains. Different from the above method, we use joint vision-language space to improve the generalization performance of models in unknown domains.

2.2. Vision-Language Models

Vision-Language Models combines models for image and natural language processing to enable understanding and interaction between images and text Du, Liu, Li and Zhao (2022). The purpose is to enable computers to understand and process both image and text data. This type of model consists of two main components: the Visual Processing Module and the Language Processing Module. Integrating visual and linguistic information enables the model to understand the semantic relationship between image and text. There are many studies on visual language pre-training models. For example, Radford et al. (2021) proposes CLIP, a contrast-based learning method that enables a joint understanding of images and text by mapping images and text into a shared embedded space so that similar images and text are closer together in that space. Reddy et al. (2021) is able to generate relevant images from natural language descriptions. It combines text description with image generation, providing users with a new, text-based way of image generation.

2.3. Word Vector

Word vector is a technique in natural language processing (NLP) that maps words to real vectors. It represents words in a continuous way, allowing for better processing of

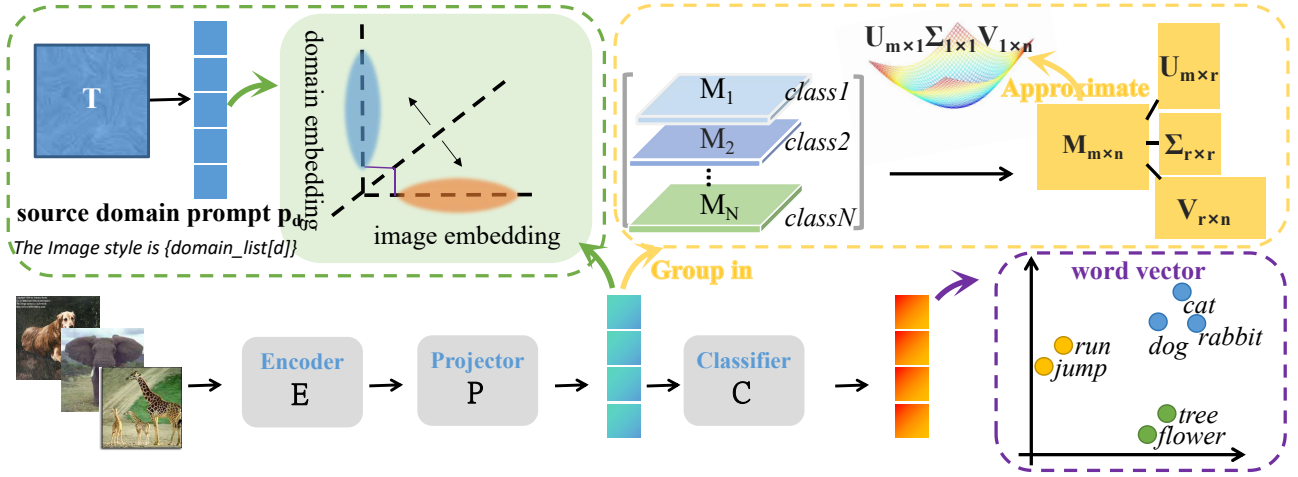


Figure 2: The framework of our proposed VLCA. The method consists of three modules, namely the domain information orthogonal decoupling module based on prompt (green dashed box), the interclass relationship constraint module based on word vectors (purple dashed box), and the intra-class feature consistency module based on low-rank space approximation (yellow dashed box).

textual information for the computer. In vector space, semantically similar words are mapped to nearby locations, so that relationships between words can be better captured. GloVe Pennington et al. (2014) and Word2Vec Church (2017) are two commonly used word vector pre-training models. Both are trained on large-scale corpus and provide pre-trained word vectors. In the paper, we use word vectors to represent the inter-class relationship of category labels.

2.4. Low-rank Matrix Decomposition

Matrix low-rank decomposition is a widely used technique in data dimensional reduction, feature extraction, and noise removal Feng and He (2017); Liu and Yan (2011); Chen, Han, Wang, Tang and Yu (2016). Traditional methods such as principal component analysis (PCA) Maćkiewicz and Ratajczak (1993) and singular value decomposition (SVD) Hoecker and Kartvelishvili (1996) have become commonly used tools to efficiently extract the main feature information of the data. SVD decomposition involves breaking down a matrix into the product of three matrices: the left singular matrix, the singular values, and the right singular matrix. In this paper, we form a matrix with features from samples of the same category and employ SVD to extract common patterns among the samples.

3. Method

We integrate language space and vision space, using the semantic space as a bridge domain, to achieve domain generalization through three modules, which are **domain information orthogonal decoupling module** in vision-language multimodal space, **word vector interclass constraint module** in language space, and **low-rank intra-class approximation module** in vision space.

In multimodal space of vision and language, the orthogonal decoupling module constrains the image feature to be orthogonal to the domain embedding, so as to suppress the

domain information in the image feature. In language space, inspired by the consistency of category semantic information in various domains, we design a module based on category relationships. Specifically, the word vector interclass constraint module provides interclass supervision by mining the semantic relations of category word vectors. In vision space, since sample features of the same category are similar and the matrix they form should be low-rank, we aggregate sample features of the same category together to form feature matrices, perform low-rank matrix decomposition, and then make the feature matrix approximate the subspace spanned by the largest singular value. The overall framework is illustrated in Fig. 2. In the following section, we first briefly introduce domain generalization, and then introduce these three key components.

3.1. Problem Definition

The domain generalization task is defined as follows: given M source domains $S_{train} = \{S_i | i = 1, \dots, M\}$, data of the i -th domain are represented as $S_i = \{x_j^i, y_j^i\}_{j=1}^{n_i}$, where x_j is the image sample and y_j is the category label. The distribution of data varies between different source domains, $P_{XY}^i \neq P_{XY}^j, 1 \leq i \neq j \leq M$. Domain generalization seeks to learn a strong generalizable function $h : \mathcal{X} \rightarrow \mathcal{Y}$ from these M source domains to minimize the error on the unseen test set, where the data distribution of target domain in test set is different from that of source domains.

3.2. Feature Decoupling Separates Domain Information

From causal analysis, as shown in Fig. 3, An image consists of two kinds of information. One is the semantic information, and the other is domain information. But the latter one is a variant factor. Only the semantic information determines the category.

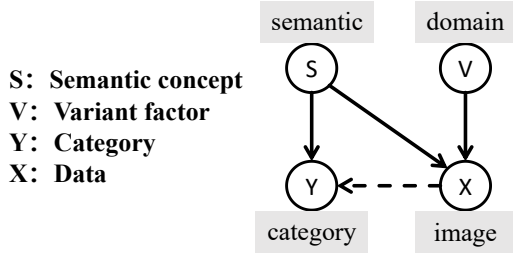


Figure 3: Causal analysis of an image. An image consists of semantic information and domain information. domain information is a variant factor. The semantic information determines the category.

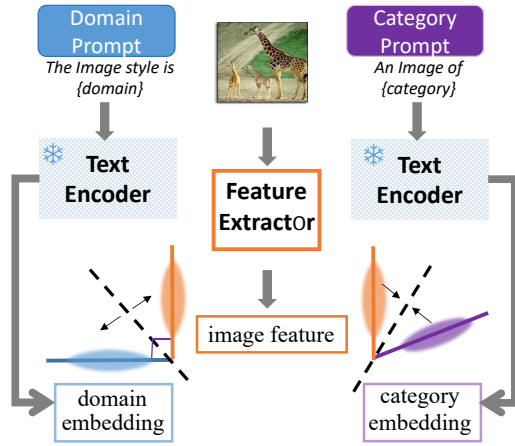


Figure 4: Feature decoupling separates domain information. The domain prompt and category prompt are fed into the feature encoder, yielding the domain embedding and category embedding, respectively. The image feature is constrained to be orthogonal to the domain embedding and aligned with the category embedding.

Therefore, for any image I belonging to domain S_j , we attempt to divide its features into two parts, namely domain-related style information and class-related semantic information. However, the image features are coupled to each other, and it is difficult to directly realize the decoupling. To address the difficulty, we relax the problem, transforming it into a projection of image feature \mathbf{F} in the directions of domain-related style information \mathbf{E}_{sty} and category-related semantic information \mathbf{E}_{sem} , as shown in Fig. 4.

The image feature \mathbf{F} is orthogonal to domain-related style information \mathbf{E}_{sty} , as formula 1.

$$\text{proj}_{\mathbf{E}_{sty}}(\mathbf{F}) = \frac{\langle \mathbf{F}, \mathbf{E}_{sty} \rangle}{\langle \mathbf{E}_{sty}, \mathbf{E}_{sty} \rangle} \mathbf{E}_{sty} \quad (1)$$

\mathbf{E}_{sty} is got by text encoder of CLIP with prompt “The Image style is {domain_list[d]}”. We expect image features \mathbf{F} and the domain-related style information embedding \mathbf{E}_{sty} to be orthogonal, which means the inner product of the domain-related style information embedding \mathbf{E}_{sty} and the image feature \mathbf{F} is zero, as shown in formula 2.

$$\langle \mathbf{F}, \mathbf{E}_{sty} \rangle = 0 \quad (2)$$

This ensures that the extracted image features do not retain domain-specific information that might influence the generalization ability of the model. Simultaneously, to make the image feature \mathbf{F} and class-related semantic information embedding \mathbf{E}_{sem} as close as possible, we apply semantic consistency supervision to constrain the angle θ of image feature \mathbf{F} and class-related semantic information embedding \mathbf{E}_{sem} being zero, which means constraining the cosine of the angle θ between these two vectors to be 1, as shown in formula 3.

$$\cos(\theta) = \frac{\mathbf{F} \cdot \mathbf{E}_{sem}}{\|\mathbf{F}\| \|\mathbf{E}_{sem}\|} = 1 \quad (3)$$

where $\|\mathbf{F}\|$ and $\|\mathbf{E}_{sem}\|$ are the norms (lengths) of \mathbf{F} and \mathbf{E}_{sem} respectively. \mathbf{E}_{sem} is got by text encoder of CLIP with prompt “An image of {category}”.

The feature decoupling loss is expressed as two parts, namely the consistent class-related loss and the orthogonal domain-related loss. The loss function is shown below.

$$\mathcal{L}_{decouple} = \mathbf{F} \cdot \mathbf{E}_{sty} + (1 - \frac{\mathbf{F} \cdot \mathbf{E}_{sem}}{\|\mathbf{F}\| \|\mathbf{E}_{sem}\|}) \quad (4)$$

3.3. Word Vector Inter-class Constraint

To further enhance the semantic supervision between categories, word vectors are used to construct semantic distributions among categories. Specifically, with the help of the pre-trained word to vector model GloVe (Global Vectors for Word Representation) Pennington et al. (2014), as shown in Fig. 5, we take each category in category set \mathcal{C} as the target category y_k and calculate the cosine distance d_{kl} between the target category y_k and other categories y_l , as in formula 5. For example, y_k is the word vector of “dog”, y_l is the word vector of “cat”, and the d_{kl} is the distance between “dog” and “cat”.

$$d_{kl} = \frac{\mathbf{y}_k \cdot \mathbf{y}_l}{\|\mathbf{y}_k\| \|\mathbf{y}_l\|}, \quad \mathbf{y}_k, \mathbf{y}_l \in \mathcal{C}, \quad (5)$$

Next, the semantic distribution of the target category y_k is constructed by normalizing the set of distances obtained by the target category and other categories and constraining their sum to 1, as shown in formula 6.

$$p_l = \frac{d_{kl}}{\sum_{j=1}^c d_{kj}}, \quad (6)$$

where c is the category number of the category set \mathcal{C} . Then, the semantic probability distribution of the target category y_k is represented as $\mathbf{P}_k = \{p_1, \dots, p_c\}$. Similarly, the semantic probability distributions for other categories are calculated. Use these distributions as supervision to calculate the semantic relationship loss $\mathcal{L}_{semantic}$ between the semantic probability distribution \mathbf{P} and the network output \mathbf{f} shown in below.

$$\mathcal{L}_{semantic} = \sum_{k=1}^m \mathbf{P}_k \log \left(\frac{\mathbf{P}_k}{\mathbf{f}_k} \right) \quad (7)$$

where m means that there are m samples in a batch.

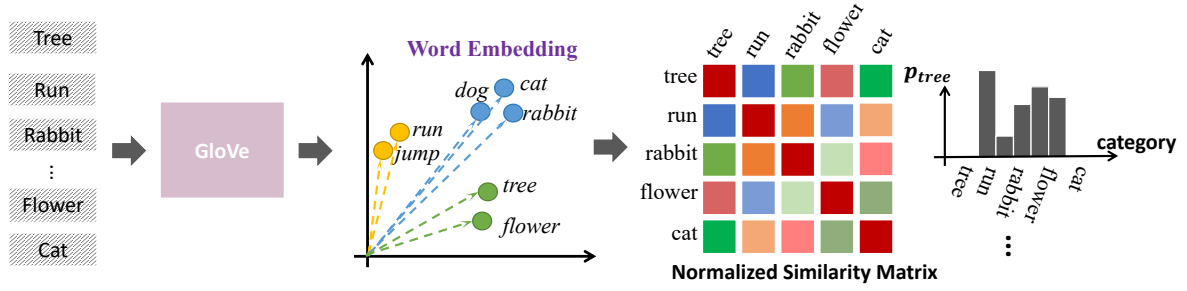


Figure 5: Word vectors construct inter-class relationship. For each category vocabulary, word vectors are obtained through GloVe. Then, the similarity matrix is calculated based on distance of these word vectors, and probability distributions are derived separately for each category.

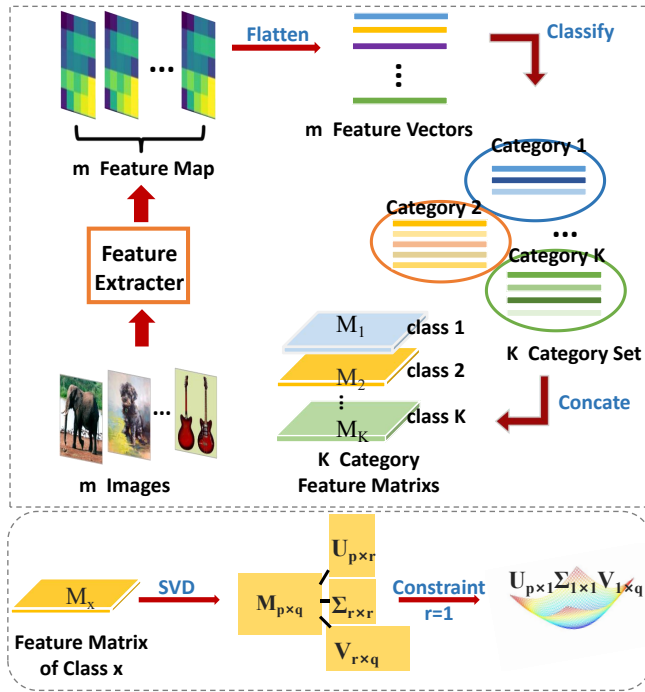


Figure 6: Low-rank decomposition realizes intra-class features constraint. Given m images as input, m feature maps are extracted by feature extractor. Then m feature maps are flattened as m feature vectors. These feature vectors are categorized into specific classes. For each class, we concatenate its vectors to form a matrix M . For any given matrix M_x , Singular Value Decomposition (SVD) is applied to obtain left singular vectors matrix U , right singular vectors matrix V^T and singular values matrix Σ . By constraining $r = 1$, enforces the inter-row correlation of the matrix M_x , thus constraining the consistency of features across different domain images of the same category to approximate the ideal feature space spanned by the largest singular value.

3.4. Low-rank Decomposition Intra-class Constraint

Although images of the same class exhibit significant differences across domains in image space, they maintain low rankness in feature space due to their feature similarity. To enhance the feature consistency within categories,

we form a matrix using the image features with the same category label in one batch.

Let \mathcal{F} be the feature matrix of a batch, where $\mathcal{F} = [\mathbf{F}_1^{l_{x_1}}, \mathbf{F}_2^{l_{x_2}}, \dots, \mathbf{F}_m^{l_{x_m}}]^T$. l_x is the category label of the feature. We perform row permutations on the feature matrix \mathcal{F} , grouping rows with the same category together, as shown in the following equation

$$\mathcal{F} = \begin{bmatrix} \mathbf{F}_1^{l_{x_1}} \\ \mathbf{F}_2^{l_{x_2}} \\ \vdots \\ \mathbf{F}_m^{l_{x_m}} \end{bmatrix} = \begin{bmatrix} \mathbf{F}_p^{l_i} \\ \vdots \\ \mathbf{F}_q^{l_j} \\ \vdots \\ \mathbf{F}_r^{l_k} \end{bmatrix} \equiv \begin{bmatrix} \mathbf{M}_i \\ \mathbf{M}_j \\ \vdots \\ \mathbf{M}_k \end{bmatrix} \quad (8)$$

where \mathbf{M}_x represents the matrix composed of sample features of the category x .

For any given category feature matrix M , applying Singular Value Decomposition (SVD) results in the factorization:

$$\mathbf{M} = \mathbf{U}\mathbf{\Sigma}\mathbf{V}^T = \sigma_1 \mathbf{u}_1 \mathbf{v}_1 + \sigma_2 \mathbf{u}_2 \mathbf{v}_2 + \dots + \sigma_r \mathbf{u}_r \mathbf{v}_r \quad (9)$$

where \mathbf{U} is the left singular matrix, $\mathbf{\Sigma}$ is the diagonal matrix of singular values, and \mathbf{V} is the right singular matrix.

Since the matrix \mathbf{M} is composed of features from the same category of images, there are common patterns among these features, resulting in shared similar feature vectors. This ultimately reduces the rank r of the matrix. Ideally, the rank of matrix \mathbf{M} should be 1.

$$\mathbf{M}_{ideal} = \sigma_1 \mathbf{u}_1 \mathbf{v}_1 = \mathbf{U}_{m \times 1} \mathbf{\Sigma}_{1 \times 1} \mathbf{V}_{1 \times n}^T \quad (10)$$

In other words, the first principal component $\mathbf{\Sigma}(1)$ carries the majority of the information in the matrix. Therefore, we constrain the matrix \mathbf{M} to approach the ideal matrix \mathbf{M}_{ideal} by imposing a constraint on the rank r of the matrix, aiming for it to approach 1. By constraining $r = 1$, achieving $rank(\mathbf{M}_x) = 1$ further enforces the inter-row correlation of the class matrix, thus constraining the consistency of features across different domain images.

$$\mathcal{L}_{approximate} = r - 1 \quad (11)$$

Combining all the loss functions together, we define full objective as:

$$\mathcal{L} = \mathcal{L}_{cls} + \alpha \cdot (\mathcal{L}_{decouple} + \mathcal{L}_{semantic}) + \beta \cdot \mathcal{L}_{approximate} \quad (12)$$

where α and β control the weights of the decouple loss and the semantic loss.

4. Experiments

We demonstrate the superiority of the proposed method on multiple DG benchmarks in this section. In addition, ablation experiments are performed on vision supervision and language constraints, respectively.

4.1. Datasets and Setting

The proposed method is evaluated on PACS Li, Yang, Song and Hospedales (2017), Office-Home Venkateswara, Eusebio, Chakraborty and Panchanathan (2017) VLCS Fang, Xu and Rockmore (2013) and TerraincognitaBeery, Van Horn and Perona (2018) DG benchmarks. We use the train-validation split following Zhou, Yang, Qiao and Xiang (2021); Zhou, Liu, Qiao, Xiang and Loy (2022). The detailed experimental parameters are set as follows. We train 50 epochs using SGD, batch size of 16, and weight decay of $5e-4$. The initial learning rate is 0.001, decreasing by 0.1 every 40 epochs. The parameter settings are the same as Carlucci, D’Innocente, Bucci, Caputo and Tommasi (2019); Zhou, Yang, Hospedales and Xiang (2020a); Xu et al. (2021). We use the image augmentation as Xu et al. (2021). Domain prompt embedding is generated by the text encoder of contrastive language-image pretraining (CLIP) Radford et al. (2021). For simplicity, we chose the “RN101” CLIP pre-trained model¹ as the text encoder. For other CLIP pre-trained text models, we show their experimental results in Section 4.3.7. The ResNet-18 and ResNet-50 pretrained on ImageNet-1k dataset are used as the backbone following previous methods. In the PACS and Office Home datasets, the prompt is “The image style is {domain}” and in the VLCS dataset, the prompt is “The image style is from dataset {domain}”. Category word vectors are obtained through pre-trained GloVe Pennington et al. (2014) models. We chose the simplest GloVe model, “glove.6B.50d”². The performance of other pre-trained word embedding models is provided in Section 4.3.6. Since the glove word vector model can only express a single lowercase word, it cannot express compound words, such as “alarm clock” in the OfficeHome dataset. Through the utilization of algebraic operations in the text embedding space (e.g. king-man+woman approaches the word representation of queen), we use the addition of two parts to express the semantic embedding of compound words. For words that are not compound words but are not retrieved, we take the approach of synonym substitution, e.g. football \Rightarrow soccer, flipflop \Rightarrow slipper. For all experiments, the α and β are set to 0.2.

4.2. Comparison with existing DG methods

4.2.1. Multi-source Domain Generalization on PACS

The results are shown in TABLE 1 and TABLE 2. Unlike other comparison methods, our proposed method achieves

optimal or suboptimal results in all domains. This is because we use dual supervision of language and vision features, which can be well constrained in the “Photo” domain and “Art” domain with rich texture and details, while the semantic information plays a good role in alignment for the more abstract and less detailed “Cartoon” domain and “Sketch” domain.

4.2.2. Multi-source Domain Generalization on OfficeHome

The results are shown in TABLE 3 and TABLE 4. The experimental results show that our method achieves competitive results, but the improvement is not obvious enough. The reason may be that, firstly, the OfficeHome dataset has 65 classes, and in order to fairly compare with other methods, we set the batch size to 16, which affects the constraints of the intraclass feature consistency module on the network. Secondly, there are many compound word labels in the dataset, and these words are not retrieved in the word vector model, which affects the network performance. As shown in Fig. 10 of Section 4.3.5, the experimental performance improves with the increase of the batch size.

4.2.3. Multi-source Domain Generalization on VLCS

The results are shown in TABLE 5. In the LabelMe dataset domain, the experimental results on ResNet 18 and ResNet 50 networks are significantly improved, with an average increase of three points. The VLCS dataset only includes 5 categories, so that more common patterns of samples of the same category can be found in low-rank approximation, so as to effectively suppress the interference factors and specific information in the image features.

4.2.4. Multi-source domain generalization on Terraincognita

The results are shown in TABLE 6. Our approach demonstrates competitive performance on long-tailed distribution datasets. This is attributed to the integration of semantic supervision via word embeddings and the text encoder, which mitigates the impact of imbalanced sample quantities. However, limitations in sample counts for certain classes hinder the effectiveness of our low-rank approximation module.

4.2.5. Single Domain Generalization Results

The results of single domain generalization on the PACS dataset using the ResNet 18 model are presented in TABLE 7. Notably, our proposed algorithm exhibits commendable performance when transferring knowledge across inherently more abstract image domains, as exemplified in the A \rightarrow S and C \rightarrow S scenarios. The noteworthy performance is attributed to the semantic result-based nature of our method. Nevertheless, it is imperative to acknowledge that the abundance of intricate textures and fine-grained details within images from the photo domain poses a challenge in the extraction of high-level semantic features. Consequently, the performance of our method in the domain transfer involving photo images is observed to be comparatively standard.

¹<https://github.com/openai/CLIP>

²<https://nlp.stanford.edu/projects/glove>

Table 1

Leave-one-domain result on PACS with ResNet-18. The best results are bolded. The second-best results are underlined.

Methods	Venue	Art	Cartoon	Photo	Sketch	Avg.
MetaRegBalaji et al. (2018)	2018 NeurIPS	83.7	77.2	95.5	70.3	81.7
JiGenCarlucci et al. (2019)	2019 CVPR	79.4	75.3	96.0	71.4	80.2
EISNetWang, Yu, Li, Fu and Heng (2020)	2020 ECCV	81.9	76.4	95.9	74.3	82.2
RSCHuang, Wang, Xing and Huang (2020)	2020 ECCV	83.4	80.3	96.0	80.9	82.2
FACTXu et al. (2021)	2021 CVPR	<u>85.4</u>	78.4	95.2	79.2	<u>84.5</u>
Pro-RandConvChoi, Das, Choi, Yang, Park and Yun (2023)	2023 CVPR	83.2	81.1	96.2	76.7	<u>84.3</u>
JVINetChu, Pan, Xu, Shi, Shi and Li (2024)	2024 PR	81.2	79.0	96.6	74.9	82.9
Ours	-	85.79	<u>80.59</u>	<u>96.29</u>	<u>80.76</u>	85.86

Table 2

Leave-one-domain result on PACS with ResNet-50. The best results are bolded. The second-best results are underlined.

Methods	Venue	Art	Cartoon	Photo	Sketch	Avg.
MetaRegBalaji et al. (2018)	2018 NeurIPS	87.2	79.2	97.6	70.3	83.6
MASFDou et al. (2019)	2019 NeurIPS	82.9	80.5	95.0	72.3	82.7
EISNetWang et al. (2020)	2020 ECCV	86.7	81.5	97.1	78.1	85.8
RSCHuang et al. (2020)	2020 ECCV	87.9	82.2	97.9	83.4	87.8
FACTXu et al. (2021)	2021 CVPR	89.6	81.8	96.7	84.5	88.2
PCLYao, Bai, Zhang, Zhang, Sun, Chen, Li and Yu (2022)	2022 CVPR	90.2	83.9	<u>98.1</u>	82.6	88.7
POEMJo and Yoon (2023)	2023 AAAI	89.4	83.0	98.2	83.2	88.5
Pro-RandConvChoi et al. (2023)	2023 CVPR	89.3	84.1	97.8	81.9	88.3
VNEKim, Kang, Hwang, Shin and Rhee (2023)	2023 CVPR	90.1	83.8	97.5	81.8	88.3
CBDMoEXu, Chen, Jia, Deng and Wang (2024)	2024 TMM	87.3	85.0	98.2	<u>85.3</u>	88.9
NormAUGQi, Yang, Shi and Geng (2024)	2024 TIP	88.9	86.0	97.2	86.0	<u>89.5</u>
HDA-LMSNg et al. (2024)	2024 NN	87.7	81.2	97.8	81.4	87.0
DBAMLi et al. (2024b)	2024 NN	<u>91.0</u>	84.0	<u>98.1</u>	83.2	89.1
Ours	-	91.94	<u>84.30</u>	97.84	84.83	89.73

Table 3

Leave-one-domain result on Office-Home with ResNet-18. The best results are bolded. The second-best results are underlined.

Method	Venue	Art	Clipart	Product	Real	Avg.
CCSAMotiian, Piccirilli, Adjero and Doretto (2017)	2017 ICCV	59.9	49.9	74.1	75.7	64.7
MMD-AAELi et al. (2018b)	2018 CVPR	56.5	47.3	72.1	74.8	62.7
JiGenCarlucci et al. (2019)	2019 CVPR	53.0	47.5	71.5	72.8	61.2
DDAIGZhou et al. (2020a)	2020 AAAI	59.2	<u>52.3</u>	74.6	<u>76.0</u>	65.5
L2A-OTZhou, Yang, Hospedales and Xiang (2020b)	2020 ECCV	60.6	50.1	74.8	77.0	65.6
RSCHuang et al. (2020)	2020 ECCV	58.4	47.9	71.6	74.5	63.1
VNEKim et al. (2023)	2023 CVPR	<u>60.4</u>	54.7	73.7	74.7	<u>65.9</u>
HDA-LMSNg et al. (2024)	2024 NN	58.5	50.8	73.4	74.5	64.3
Ours	-	59.33	56.45	<u>74.16</u>	74.94	66.2

Table 4

Leave-one-domain result on Office-Home with ResNet-50. The best results are bolded. The second-best results are underlined.

Method	Venue	Art	Clipart	Product	Real	Avg.
RSCHuang et al. (2020)	2020 ECCV	60.7	51.4	74.8	75.1	65.5
MMDLi et al. (2018b)	2018 CVPR	60.4	53.3	74.3	77.4	66.4
MTLBlanchard, Deshmukh, Dogan, Lee and Scott (2021)	2021 JMLR	61.5	52.4	74.9	76.8	66.4
VRExKrueger, Caballero, Jacobsen, Zhang, Binas, Zhang, Le Priol and Courville (2021)	2021 ICML	60.7	53.0	75.3	76.6	66.4
MLDGLi et al. (2018a)	2018 AAAI	61.5	53.2	75.0	77.5	66.8
I-MixupXu, Zhang, Ni, Li, Wang, Tian and Zhang (2020)	2020 AAAI	62.4	54.8	76.9	78.3	68.1
SagNetNam, Lee, Park, Yoon and Yoo (2021)	2021 CVPR	63.4	54.8	75.8	78.3	68.1
SWADCha, Chun, Lee, Cho, Park, Lee and Park (2021)	2021 NeurIPS	<u>66.1</u>	57.7	78.4	<u>80.2</u>	70.6
POEMJo and Yoon (2023)	2023 AAAI	64.1	53.9	76.2	77.6	68.0
VNEKim et al. (2023)	2023 CVPR	66.6	<u>58.6</u>	78.9	80.5	<u>71.1</u>
JVINetChu et al. (2024)	2024 PR	-	-	-	-	68.3
Ours	-	65.43	61.37	<u>78.55</u>	79.25	71.15

Table 5

Leave-one-domain result on VLCS with ResNet-18 and ResNet-50. The best results are bolded.

Method	Venue	C	L	S	V	Avg.
ResNet 18						
DeepAllZhou et al. (2020a)	2020 AAAI	91.9	61.8	68.8	67.5	72.5
RSCHuang et al. (2020)	2020 ECCV	95.8	63.7	72.1	71.9	75.9
MMLDMatsuura and Harada (2020)	2020 AAAI	97.0	62.2	<u>72.5</u>	73.0	76.2
StableNetZhang, Cui, Xu, Zhou, He and Shen (2021)	2021 CVPR	96.7	65.4	75.0	73.6	77.7
MVDGZhang, Qi, Shi and Gao (2022)	2022 ECCV	98.4	63.8	71.1	75.3	77.2
VNEKim et al. (2023)	2023 CVPR	97.5	<u>65.9</u>	70.4	78.4	<u>78.1</u>
Ours	-	<u>97.88</u>	68.30	72.46	<u>75.89</u>	78.63
ResNet 50						
VNEKim et al. (2023)	2023 CVPR	99.2	63.7	74.4	81.6	79.7
JVINetChu et al. (2024)	2024 PR	-	-	-	-	79.1
Ours	-	98.80	67.78	77.12	78.41	80.53

Table 6

Leave-one-domain result on Terraincognita with ResNet-50. The best results are bolded.

Method	Venue	Location100	Location38	Location43	Location46	Avg
RSCHuang et al. (2020)	2020 ECCV	50.2	39.2	56.3	<u>40.8</u>	46.6
I-MixupXu et al. (2020)	2020 AAAI	59.6	42.2	55.9	33.9	47.9
VRExKrueger et al. (2021)	2021 ICML	48.2	41.7	56.8	38.7	46.4
SagNetNam et al. (2021)	2021 CVPR	53.0	43.0	57.9	40.4	48.6
SWADChattopadhyay, Balaji and Hoffman (2020)	2021 NeurIPS	55.4	44.9	<u>59.7</u>	39.9	50.0
RatatouilleRame, Ahuja, Zhang, Cord, Bottou and Lopez-Paz (2023)	2023 CVPR	<u>57.9</u>	50.6	60.2	39.2	52.0
JVINetChu et al. (2024)	2024 PR	-	-	-	-	46.8
Ours	-	59.61	<u>44.96</u>	57.08	42.14	<u>50.94</u>

4.3. Ablation Study and Analysis

4.3.1. Impact of different components

We perform a comprehensive ablation study to examine the contribution of each component within our model, as detailed in TABLE 8. Beginning with baseline, model A is with word vector semantic module. Model D is with word vector semantic module and CLIP domain information decouple module. The proposed method is all with word vector semantic module, CLIP domain information decouple module and same-category-feature approximation module.

4.3.2. 3D t-SNE Visualization on Category

The 3D t-SNE visualization of leave-one-domain models in Cartoon domain on PACS with ResNet 18 is shown in Fig. 7. From the t-SNE visualization, it is evident that samples belonging to the “dog” category share close feature space with those from the “horse” category. Similarly, the

relationship between “elephant” and “giraffe” appears to be proximate, while “person” and “house” also exhibit a close association. These observed correspondences align well with the semantic representations in the word vectors, validating their consistent semantic relevance.

4.3.3. t-SNE Visualization on Data Doamin

We show the t-SNE visualization on different data domain features in Fig. 8. It can be seen that data from the four domains are mix up with each other according to categories.

4.3.4. Feature Heatmap Visualization

The heatmap results for the ResNet 50 model on the VLCS dataset are presented in Fig. 9. This figure provides an overview of the feature heatmaps for images spanning four distinct domains and five diverse categories. This emphasis aligns with the presence of class-specific features that

Table 7

Single-source Domain Generalization on PACS with ResNet-18. (A: Art Painting, C: Cartoon, S: Sketch, P: Photo). JiGen Carlucci et al. (2019) results are reproduced with their official code. ADA Volpi, Namkoong, Sener, Duchi, Murino and Savarese (2018) and SagNet Nam et al. (2021) results are reported based on implementations from Nam et al. (2021).

Methods	Venue	A→C	A→S	A→P	C→A	C→S	C→P	S→A	S→C	S→P	P→A	P→C	P→S	Avg.
JiGen Carlucci et al. (2019)	2019 CVPR	57.0	50.0	96.1	65.3	65.9	85.5	26.6	41.1	42.8	62.4	27.2	35.5	54.6
ADA Volpi et al. (2018)	2018 NeurIPS	64.3	58.5	94.5	66.7	65.6	83.6	37.0	58.6	41.6	65.3	32.7	35.9	58.7
SagNet Nam et al. (2021)	2021 CVPR	67.1	56.8	95.7	72.1	69.2	85.7	41.1	62.9	46.2	69.8	35.1	40.7	61.9
GeoTexAug Liu, Yang and Hall (2022)	2022 CVPR	67.4	51.7	97.1	79.8	66.4	89.9	50.6	70.5	58.8	69.4	38.7	39.1	65.0
Ours	-	65.70	65.18	96.11	77.25	70.73	87.49	52.44	62.54	55.15	66.06	34.98	44.95	64.88

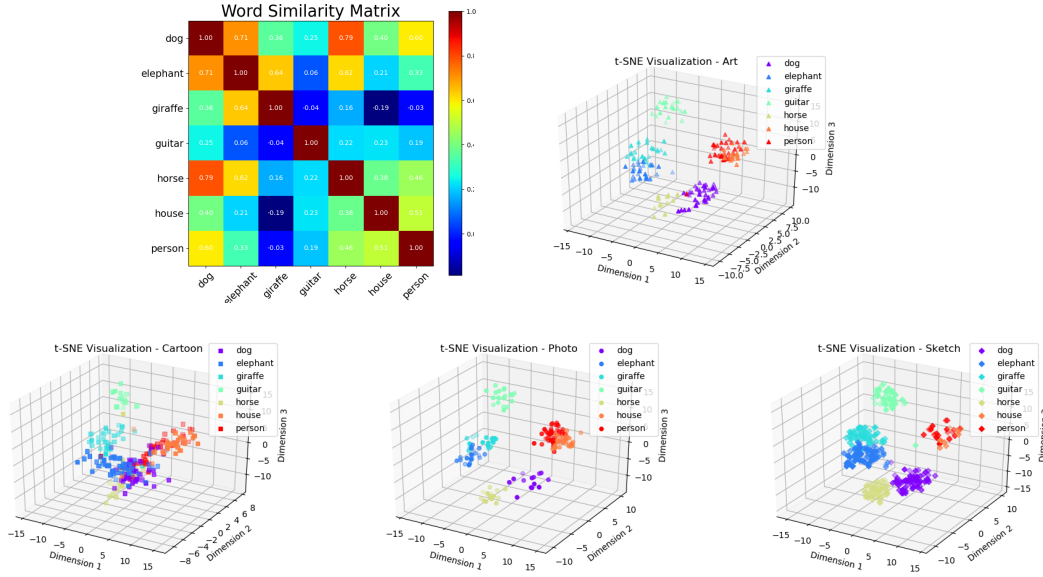


Figure 7: The 3D t-SNE visualization of leave-one-domain models on PACS with ResNet 18. The leave-one-domain is set to Art. It can be visually observed that the features of giraffe are close to the features of epephant, as their word vectors are close.

Table 8

Ablation study. We study the influence of three different components of our method. cls: the classification loss, semantic: word vectors inter-class supervision module, decouple: domain embedding orthogonal decouple module, approximate: feature matrix approximate module.

Model Component				Target Domain Accuracy (%)
Method	$\mathcal{L}_{semantic}$	$\mathcal{L}_{decouple}$	$\mathcal{L}_{approximate}$	Avg.
Baseline	-	-	-	80.16
Model A	✓	-	-	84.35
Model D	✓	✓	-	84.91
Ours	✓	✓	✓	85.86

hold discriminative significance. The discernible correlation between the network’s focus and these distinctive features underscores the model’s ability to recognize and highlight meaningful patterns.

4.3.5. Ablation Study on Batchsize

We conduct experiments with different batch sizes as shown in Fig. 10. Specifically, experiments are conducted with batch sizes of 8, 16, 32, and 64. Due to limitations in GPU memory, we are unable to test larger batch sizes. The experimental results indicate a continuous improvement in overall performance as the batch size increases. This can be attributed to the fact that with larger batch sizes, the low-rank approximate module for intra-class consistency constraints can identify more shared patterns among samples from different domains but of the same class. Consequently, this leads to a reduction in inter-domain disparities, an increase in intra-class differences, and an enhancement in

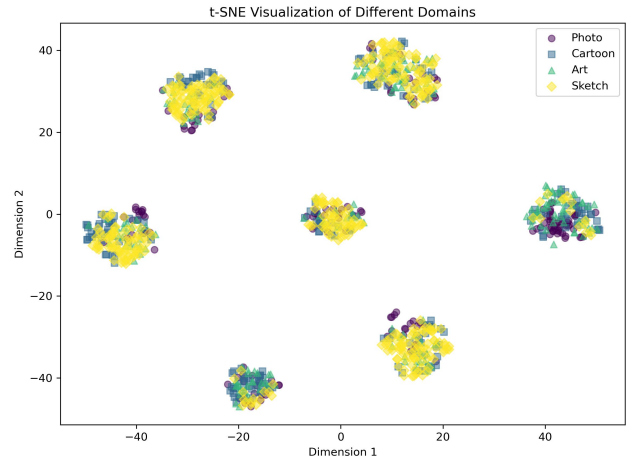


Figure 8: The distribution of the source and the target data.

the robustness and generalization capabilities of the model. The main body of the Clipart dataset clearly has minimal background interference. The reason for the decrease in performance on Clipart domain may be that when the batch size increases, the background information from images in other domains may interfere with the features of the Clipart domain images.

4.3.6. Ablation Study on Word Vector Model

To explore the influence of word vector models on performance, we conduct tests using open-source word vector models, including GloVe and Word2Vec as shown in TABLE 9. The experimental results reveal that “glove.42B.300d” outperforms the others. This can be attributed to the fact that

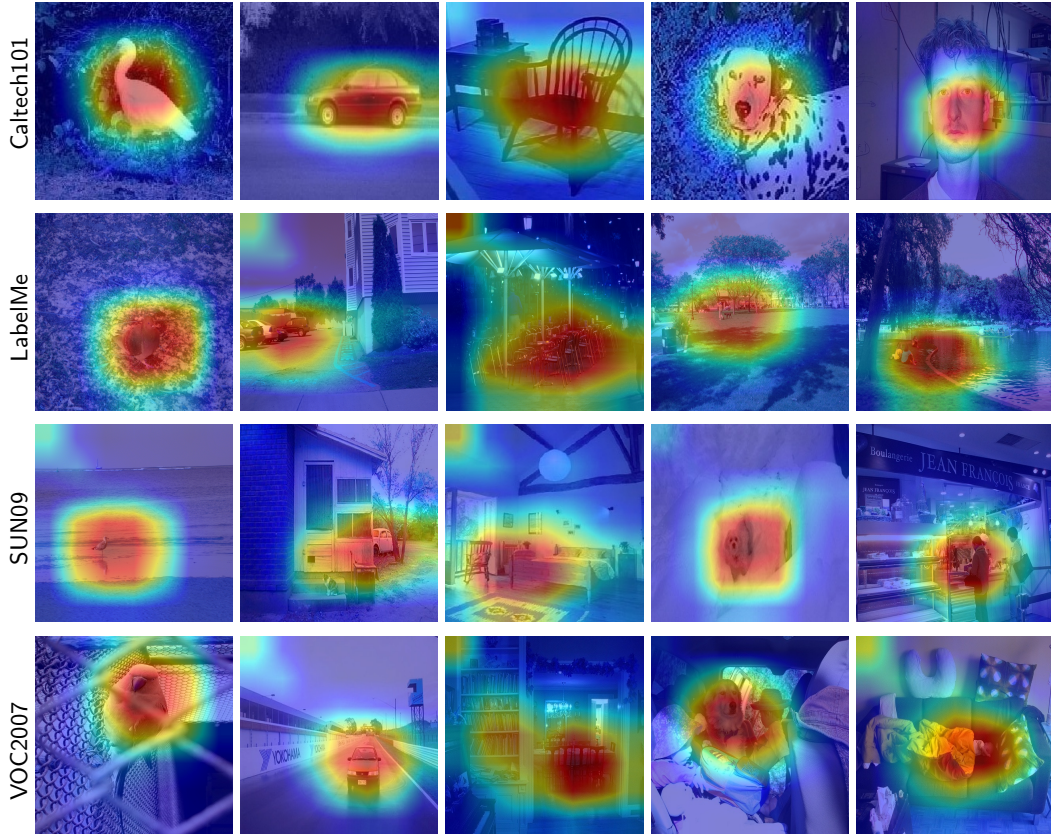


Figure 9: The feature visualization of leave-one-domain models on VLCS with ResNet-50. The leave-one-domain is set to LabelMe. Each image is composed of the original image overlaid with its corresponding feature heatmap. In the heatmap, red corresponds to positions with high feature values, while blue corresponds to positions with lower feature values.

Table 9

The leave-one-domain results by using different word vector model on VLCS with ResNet-50.

Word Vector Model	C	L	S	V	Avg.
glove.6B.50d	98.80	67.78	77.12	78.41	80.53
glove.6B.100d	99.29	68.60	74.62	78.29	80.20
glove.6B.200d	99.08	66.98	76.36	78.44	80.22
glove.6B.300d	98.94	67.51	76.64	78.82	80.48
glove.42B.300d	99.01	67.77	77.06	79.06	80.73
glove.twitter.27B.25d	98.80	67.24	75.62	79.59	80.31
GoogleNews-vectors-negative300	98.73	67.28	75.93	78.70	80.16

this model is based on a large corpus and employs high-dimensional representations for each word, enabling fine-grained characterization.

4.3.7. Ablation Study on CLIP Prtrained Model

To compare the impact of CLIP pre-trained models on domain prompt encoding, we conduct tests on different pre-trained models, and the results are shown in TABLE 10. The experimental findings indicate that RN50x16 demonstrates the best overall performance, outperforming other models.

Table 10

The leave-one-domain results by using different CLIP pre-trained models on VLCS with ResNet-50.

CLIP pre-trained model	C	L	S	V	Avg.
RN50	98.94	66.38	76.75	78.02	80.02
RN101	98.80	67.78	77.12	78.41	80.53
RN50x4	98.87	67.85	76.20	77.87	80.20
RN50x16	98.73	70.26	76.23	78.23	80.86
ViT-B/32	98.94	67.39	75.26	78.52	80.03
ViT-B/16	99.08	67.21	74.89	80.27	80.36
ViT-L/14	99.15	68.83	76.45	76.78	80.30
ViT-L/14@336px	99.22	68.11	75.50	79.32	80.54

5. Conclusion

In this paper, we combine language space and image space, using semantic space as the bridge domain, to explore the generalization ability of models in unknown target domains. In the language space, relative relationships between categories are explored through word vectors. In image space, the common pattern among sample features of the same category is sought by mapping the feature matrix to the low-rank subspace. In multimodal space, domain-related image features are removed through CLIP-based text domain prompts. Given the current state of incompleteness

With the ongoing advancements in natural language processing, it is expected that language models will offer more robust supervision, thereby enhancing domain generalization capabilities. In addition, image basic units with semantic properties are also worth exploring. Based on the above, with the development of large language models and the further improvement of GPU memory, the performance of the proposed method has room for further improvement.

References

- Balaji, Y., Sankaranarayanan, S., Chellappa, R., 2018. Metareg: Towards domain generalization using meta-regularization. *Advances in neural information processing systems* 31.
- Beery, S., Van Horn, G., Perona, P., 2018. Recognition in terra incognita, in: *Proceedings of the European conference on computer vision (ECCV)*, pp. 456–473.
- Blanchard, G., Deshmukh, A.A., Dogan, Ü., Lee, G., Scott, C., 2021. Domain generalization by marginal transfer learning. *The Journal of Machine Learning Research* 22, 46–100.
- Carlucci, F.M., D’Innocente, A., Bucci, S., Caputo, B., Tommasi, T., 2019. Domain generalization by solving jigsaw puzzles, in: *Proceedings of the IEEE/CVF Conference on Computer Vision and Pattern Recognition*, pp. 2229–2238.
- Cha, J., Chun, S., Lee, K., Cho, H.C., Park, S., Lee, Y., Park, S., 2021. Swad: Domain generalization by seeking flat minima. *Advances in Neural Information Processing Systems* 34, 22405–22418.
- Chaari, M., Fekih, A., Seibi, A.C., Hmida, J.B., 2018. A frequency-domain approach to improve anns generalization quality via proper initialization. *Neural Networks* 104, 26–39.
- Chattopadhyay, P., Balaji, Y., Hoffman, J., 2020. Learning to balance specificity and invariance for in and out of domain generalization, in: *European Conference on Computer Vision*, Springer. pp. 301–318.
- Chen, X., Han, Z., Wang, Y., Tang, Y., Yu, H., 2016. Nonconvex plus quadratic penalized low-rank and sparse decomposition for noisy image alignment. *Sci. China Inf. Sci.* 59, 052107–1.
- Choi, S., Das, D., Choi, S., Yang, S., Park, H., Yun, S., 2023. Progressive random convolutions for single domain generalization, in: *Proceedings of the IEEE/CVF Conference on Computer Vision and Pattern Recognition*, pp. 10312–10322.
- Chu, J.Z., Pan, B., Xu, X., Shi, T.Y., Shi, Z.W., Li, T., 2024. Joint variational inference network for domain generalization. *Pattern Recognition* , 110587.
- Church, K.W., 2017. Word2vec. *Natural Language Engineering* 23, 155–162.
- Dou, Q., Coelho de Castro, D., Kamnitsas, K., Glocker, B., 2019. Domain generalization via model-agnostic learning of semantic features. *Advances in neural information processing systems* 32.
- Du, Y., Liu, Z., Li, J., Zhao, W.X., 2022. A survey of vision-language pre-trained models .
- Du, Y., Xu, J., Xiong, H., Qiu, Q., Zhen, X., Snoek, C.G., Shao, L., 2020. Learning to learn with variational information bottleneck for domain generalization, in: *Computer Vision–ECCV 2020: 16th European Conference, Glasgow, UK, August 23–28, 2020, Proceedings, Part X* 16, Springer. pp. 200–216.
- Fang, C., Xu, Y., Rockmore, D.N., 2013. Unbiased metric learning: On the utilization of multiple datasets and web images for softening bias, in: *Proceedings of the IEEE International Conference on Computer Vision*, pp. 1657–1664.
- Feng, X., He, X., 2017. Robust low-rank data matrix approximations. *Science China Mathematics* 60, 189–200.
- Floridi, L., Chiriatti, M., 2020. Gpt-3: Its nature, scope, limits, and consequences. *Minds and Machines* 30, 681–694.
- Ge, F., Zhang, Y., Wang, L., Coleman, S., Kerr, D., 2023. Double-domain adaptation semantics for retrieval-based long-term visual localization. *IEEE Transactions on Multimedia* , 1–16doi:10.1109/TMM.2023.3345138.

Figure 10: The leave-one-domain results on OfficeHome with ResNet-50 under different batchsize.

in language models, the experiment results have achieved competitive performance.

6. Limitation and Discussion

Though our algorithm has good performance on the dataset, the proposed three modules still have limitations. Firstly, The domain information orthogonal decoupling module is implemented based on the semantic prompt of the CLIP pre-trained model. This requires that the semantic prompt be meaningful, that is, the domain features are clear, such as rain, fog, cartoons, sketches, etc. However, for datasets with unclear domain information, such as Digits or VLCS, the effect is reduced. Secondly, word vector inter-class constraint module is limited by the completeness of the word vector model. When the category words in the dataset cannot be retrieved in the word vector model, the semantics of the substitute words may be different from that of the original category words, which reduces the accuracy of the interclass relationship. At last, the low-rank decomposition intra-class constraint module is affected by batch size. Since the purpose of this module is to find common feature patterns of the same category samples, larger batch sizes have been shown to achieve better results.

- Hoecker, A., Kartvelishvili, V., 1996. Svd approach to data unfolding. *Nuclear Instruments and Methods in Physics Research Section A: Accelerators, Spectrometers, Detectors and Associated Equipment* 372, 469–481.
- Huang, Z., Wang, H., Xing, E.P., Huang, D., 2020. Self-challenging improves cross-domain generalization, in: *Computer Vision–ECCV 2020: 16th European Conference, Glasgow, UK, August 23–28, 2020, Proceedings, Part II* 16, Springer. pp. 124–140.
- Jia, L., Chow, T.W., Yuan, Y., 2024. Causal disentanglement domain generalization for time-series signal fault diagnosis. *Neural Networks* 172, 106099.
- Jo, S.Y., Yoon, S.W., 2023. Poem: polarization of embeddings for domain-invariant representations. *Association for the Advancement of Artificial Intelligence (AAAI)*.
- Kang, J., Lee, S., Kim, N., Kwak, S., 2022. Style neophile: Constantly seeking novel styles for domain generalization, in: *Proceedings of the IEEE/CVF Conference on Computer Vision and Pattern Recognition*, pp. 7130–7140.
- Kim, J., Kang, S., Hwang, D., Shin, J., Rhee, W., 2023. Vne: An effective method for improving deep representation by manipulating eigenvalue distribution, in: *Proceedings of the IEEE/CVF Conference on Computer Vision and Pattern Recognition*, pp. 3799–3810.
- Krueger, D., Caballero, E., Jacobsen, J.H., Zhang, A., Binas, J., Zhang, D., Le Priol, R., Courville, A., 2021. Out-of-distribution generalization via risk extrapolation (rex), in: *International Conference on Machine Learning*, PMLR. pp. 5815–5826.
- Li, D., Yang, Y., Song, Y.Z., Hospedales, T., 2018a. Learning to generalize: Meta-learning for domain generalization, in: *Proceedings of the AAAI conference on artificial intelligence*.
- Li, D., Yang, Y., Song, Y.Z., Hospedales, T.M., 2017. Deeper, broader and artier domain generalization, in: *Proceedings of the IEEE international conference on computer vision*, pp. 5542–5550.
- Li, H., Pan, S.J., Wang, S., Kot, A.C., 2018b. Domain generalization with adversarial feature learning, in: *Proceedings of the IEEE conference on computer vision and pattern recognition*, pp. 5400–5409.
- Li, J., Cheng, B., Chen, Y., Gao, G., Shi, J., Zeng, T., 2024a. Ewt: Efficient wavelet-transformer for single image denoising. *Neural Networks*, 106378.
- Li, J., Li, Y., Tan, J., Liu, C., 2024b. It takes two: Dual branch augmentation module for domain generalization. *Neural Networks* 172, 106094.
- Lin, G., Bao, Z., Huang, Z., Li, Z., Zheng, W.s., Chen, Y., 2024. A multi-level relation-aware transformer model for occluded person re-identification. *Neural Networks*, 106382.
- Liu, G., Yan, S., 2011. Latent low-rank representation for subspace segmentation and feature extraction, in: *2011 international conference on computer vision*, IEEE. pp. 1615–1622.
- Liu, X.C., Yang, Y.L., Hall, P., 2022. Geometric and textural augmentation for domain gap reduction, in: *Proceedings of the IEEE/CVF Conference on Computer Vision and Pattern Recognition*, pp. 14340–14350.
- Liu, Y., Xiong, Z., Li, Y., Tian, X., Zha, Z.J., 2021. Domain generalization via encoding and resampling in a unified latent space. *IEEE Transactions on Multimedia* 25, 126–139.
- Liu, Z., Lv, Q., Lee, C.H., Shen, L., 2024. Segmenting medical images with limited data. *Neural Networks*, 106367.
- MacKiewicz, A., Ratajczak, W., 1993. Principal components analysis (pca). *Computers & Geosciences* 19, 303–342.
- Matsuura, T., Harada, T., 2020. Domain generalization using a mixture of multiple latent domains, in: *Proceedings of the AAAI Conference on Artificial Intelligence*, pp. 11749–11756.
- Motian, S., Piccirilli, M., Adjeroh, D.A., Doretto, G., 2017. Unified deep supervised domain adaptation and generalization, in: *Proceedings of the IEEE international conference on computer vision*, pp. 5715–5725.
- Muandet, K., Balduzzi, D., Schölkopf, B., 2013. Domain generalization via invariant feature representation, in: *International conference on machine learning*, PMLR. pp. 10–18.
- Nam, H., Lee, H., Park, J., Yoon, W., Yoo, D., 2021. Reducing domain gap by reducing style bias, in: *Proceedings of the IEEE/CVF Conference on Computer Vision and Pattern Recognition*, pp. 8690–8699.
- Ng, W.W., Zhang, Q., Zhong, C., Zhang, J., 2024. Improving domain generalization by hybrid domain attention and localized maximum sensitivity. *Neural Networks* 171, 320–331.
- Niu, Z., Yuan, J., Ma, X., Xu, Y., Liu, J., Chen, Y.W., Tong, R., Lin, L., 2023. Knowledge distillation-based domain-invariant representation learning for domain generalization. *IEEE Transactions on Multimedia*.
- Pennington, J., Socher, R., Manning, C.D., 2014. Glove: Global vectors for word representation, in: *Proceedings of the 2014 conference on empirical methods in natural language processing (EMNLP)*, pp. 1532–1543.
- Qi, L., Yang, H., Shi, Y., Geng, X., 2024. Normaug: Normalization-guided augmentation for domain generalization. *IEEE Transactions on Image Processing* 33, 1419–1431.
- Radford, A., Kim, J.W., Hallacy, C., Ramesh, A., Goh, G., Agarwal, S., Sastry, G., Askell, A., Mishkin, P., Clark, J., et al., 2021. Learning transferable visual models from natural language supervision, in: *International conference on machine learning*, PMLR. pp. 8748–8763.
- Rame, A., Ahuja, K., Zhang, J., Cord, M., Bottou, L., Lopez-Paz, D., 2023. Model ratatouille: Recycling diverse models for out-of-distribution generalization. *International Conference on Machine Learning*.
- Reddy, M.D.M., Basha, M.S.M., Hari, M.M.C., Penchalaiah, M.N., 2021. Dall-e: Creating images from text. *UGC Care Group I Journal* 8, 71–75.
- Tian, Y., Li, J., Fu, H., Zhu, L., Yu, L., Wan, L., 2024. Self-mining the confident prototypes for source-free unsupervised domain adaptation in image segmentation. *IEEE Transactions on Multimedia*, 1–11doi:10.1109/TMM.2024.3370678.
- Venkateswara, H., Eusebio, J., Chakraborty, S., Panchanathan, S., 2017. Deep hashing network for unsupervised domain adaptation, in: *Proceedings of the IEEE conference on computer vision and pattern recognition*, pp. 5018–5027.
- Volpi, R., Namkoong, H., Sener, O., Duchi, J.C., Murino, V., Savarese, S., 2018. Generalizing to unseen domains via adversarial data augmentation. *Advances in neural information processing systems* 31.
- Wang, S., Yu, L., Li, C., Fu, C.W., Heng, P.A., 2020. Learning from extrinsic and intrinsic supervisions for domain generalization, in: *European Conference on Computer Vision*, Springer. pp. 159–176.
- Wu, H., Liu, J., Zha, Z.J., Chen, Z., Sun, X., 2019a. Mutually reinforced spatio-temporal convolutional tube for human action recognition., in: *IJCAI*, pp. 968–974.
- Wu, H., Liu, J., Zhu, X., Wang, M., Zha, Z.J., 2021. Multi-scale spatial-temporal integration convolutional tube for human action recognition, in: *Proceedings of the Twenty-Ninth International Conference on International Joint Conferences on Artificial Intelligence*, pp. 753–759.
- Wu, H., Zha, Z.J., Wen, X., Chen, Z., Liu, D., Chen, X., 2019b. Cross-fiber spatial-temporal co-enhanced networks for video action recognition, in: *Proceedings of the 27th ACM international conference on multimedia*, pp. 620–628.
- Xu, F., Chen, D., Jia, T., Deng, S., Wang, H., 2024. Cbdmoec: Consistent-but-diverse mixture of experts for domain generalization. *IEEE Transactions on Multimedia*.
- Xu, M., Zhang, J., Ni, B., Li, T., Wang, C., Tian, Q., Zhang, W., 2020. Adversarial domain adaptation with domain mixup, in: *Proceedings of the AAAI Conference on Artificial Intelligence*, pp. 6502–6509.
- Xu, Q., Zhang, R., Zhang, Y., Wang, Y., Tian, Q., 2021. A fourier-based framework for domain generalization, in: *Proceedings of the IEEE/CVF Conference on Computer Vision and Pattern Recognition*, pp. 14383–14392.
- Yao, X., Bai, Y., Zhang, X., Zhang, Y., Sun, Q., Chen, R., Li, R., Yu, B., 2022. Pcl: Proxy-based contrastive learning for domain generalization, in: *Proceedings of the IEEE/CVF Conference on Computer Vision and Pattern Recognition*, pp. 7097–7107.
- Zhang, J., Qi, L., Shi, Y., Gao, Y., 2022. Mvdg: A unified multi-view framework for domain generalization, in: *European Conference on Computer Vision*, Springer. pp. 161–177.
- Zhang, J., Rao, Y., Huang, X., Li, G., Zhou, X., Zeng, D., 2024. Frequency-aware multi-modal fine-tuning for few-shot open-set remote sensing scene classification. *IEEE Transactions on Multimedia*, 1–15doi:10.1109/TMM.2024.3372416.

- Zhang, X., Cui, P., Xu, R., Zhou, L., He, Y., Shen, Z., 2021. Deep stable learning for out-of-distribution generalization, in: Proceedings of the IEEE/CVF Conference on Computer Vision and Pattern Recognition, pp. 5372–5382.
- Zhou, F., Chen, Y., Yang, S., Wang, B., Chaib-Draa, B., 2023. On the value of label and semantic information in domain generalization. *Neural Networks* 163, 244–255.
- Zhou, K., Liu, Z., Qiao, Y., Xiang, T., Loy, C.C., 2022. Domain generalization: A survey. *IEEE Transactions on Pattern Analysis and Machine Intelligence*.
- Zhou, K., Yang, Y., Hospedales, T., Xiang, T., 2020a. Deep domain-adversarial image generation for domain generalisation, in: Proceedings of the AAAI conference on artificial intelligence, pp. 13025–13032.
- Zhou, K., Yang, Y., Hospedales, T., Xiang, T., 2020b. Learning to generate novel domains for domain generalization, in: *Computer Vision–ECCV 2020: 16th European Conference, Glasgow, UK, August 23–28, 2020, Proceedings, Part XVI* 16, Springer. pp. 561–578.
- Zhou, K., Yang, Y., Qiao, Y., Xiang, T., 2021. Domain adaptive ensemble learning. *IEEE Transactions on Image Processing* 30, 8008–8018.
- Zhu, X., Liu, J., Wu, H., Wang, M., Zha, Z.J., 2020. Asta-net: Adaptive spatio-temporal attention network for person re-identification in videos, in: Proceedings of the 28th ACM International Conference on Multimedia, pp. 1706–1715.